This is the accepted manuscript made available via CHORUS. The article has been published as:

Applications of reduced-basis methods to the nuclear single-particle spectrum

Amy L. Anderson, Graham L. O'Donnell, and J. Piekarewicz

Phys. Rev. C **106**, L031302 — Published 30 September 2022

DOI: 10.1103/PhysRevC.106.L031302

Applications of reduced basis methods to the nuclear single-particle spectrum

Amy L. Anderson,* Graham L. O'Donnell,† and J. Piekarewicz‡
Department of Physics, Florida State University, Tallahassee, FL 32306, USA
(Dated: September 12, 2022)

Reduced basis methods provide a powerful framework for building efficient and accurate emulators. Although widely applied in many fields to simplify complex models, reduced basis methods have only been recently introduced into nuclear physics. In this letter we build an emulator to study the single-particle structure of atomic nuclei. By scaling a suitable mean-field Hamiltonian, a "universal" reduced basis is constructed capable of accurately and efficiently reproduce the entire single-particle spectrum of a variety of nuclei. Indeed, the reduced basis model reproduces both ground- and excited-state energies as well as the associated wave-functions with remarkable accuracy. Our results bode well for more demanding applications that use Bayesian optimization to calibrate nuclear energy density functionals.

Eigenvector continuation (EC) is a novel method for calculating eigenstates of a Hamiltonian matrix defined by one or more variable parameters [1]. The core assumption behind the success of EC is that eigenstates vary smoothly over the manifold defined by the parameters, so that the eigenstates for a given parameter are likely to be well approximated by a linear combination of the eigenstates obtained with another set of parameters. Where a direct calculation of eigenstates—such as direct matrix diagonalization in large vector spaces—would be computationally demanding, EC transforms the problem into a simple diagonalization in a low-dimensional space. The nuclear physics community has benefited greatly from these new insights and has developed a set of accurate and efficient emulators using eigenvector continuation [2–4].

Recently, EC has been identified to belong to a general class of techniques that fall under the general rubric of "reduced basis methods" (RBMs) [5, 6]. Although new to nuclear physics [7, 8], reduced basis methods—as part of the general framework of reduced order models [9]—is a relatively mature field that offers efficient and accurate solutions to numerically challenging problems over a wide scientific landscape [9]. It is the goal of this letter to continue the application of RBMs to nuclear science, particularly in the context of the independent particle model.

The independent particle model is a fundamental pillar of nuclear structure. As argued by Bohr and Mottelson: "the relatively long mean free path of the nucleons implies that the interactions primarily contribute a smoothly varying average potential in which the particles move independently" [10]. Self-consistent mean-field models that are at the core of nuclear energy density functionals exploit this paradigm to find the optimal set of single particle orbitals. Even more sophisticated models, such as ab initio no core shell model and coupled cluster theory often start from a simple single-particle basis that preserves translational symmetry [11] or from a reference state that consists of a Slater determinant of single-particle orbitals that gets refined by the inclusion of many-body correlations [12].

* aanderson6@fsu.edu
† glo15@fsu.edu
‡ jpiekarewicz@fsu.edu

Despite the remarkable advances in algorithmic development, computer power, and physical insights, diagonalizing Hamiltonian matrices in model spaces containing millions of basis states is often required. As such, reduced basis methods can provide a framework to drastically increase computational speed while retaining accuracy. RBMs have only been recently introduced into nuclear physics, so many questions remain on its applicability to the many difficult problems permeating the field. In this work we demonstrate how RBMs can generate a "universal" set of basis states that may be used to compute the entire single-particle spectrum—both ground and excited states—of a variety of nuclei across the nuclear chart.

To start, we introduce a dimensionless Schrödinger equation in the presence of a spherically symmetric mean-field Hamiltonian $\hat{H}|\mathcal{U}_{n\kappa}\rangle = \varepsilon|\mathcal{U}_{n\kappa}\rangle$, which in configuration space turns into the following second-order differential equation:

$$\left(-\frac{d^2}{dx^2} + V(x) + \frac{\kappa(\kappa+1)}{x^2}\right)\mathcal{U}_{n\kappa}(x) = \varepsilon\,\mathcal{U}_{n\kappa}(x). \tag{1}$$

Here ε is the dimensionless energy to be defined later and κ is a shorthand notation for both the total angular momentum $j = |\kappa| - 1/2$ and the orbital angular momentum l

$$l = \begin{cases} \kappa & \text{if } \kappa > 0 \\ -(1+\kappa) & \text{if } \kappa < 0. \end{cases} \tag{2}$$

Note that $\kappa(\kappa+1) = l(l+1)$. The spherically symmetric mean-field potential $V(x)$ includes central, Coulomb, and spin-orbit contributions that are parametrized in terms of a Woods-Saxon potential, a Coulomb potential derived from an assumed Gaussian charge distribution, and the derivative of a Woods-Saxon potential, respectively. That is,

$$V(x) = -\lambda_0 f_0(x) + \lambda_c f_c(x) + (1+\kappa)\lambda_{so} f_{so}(x), \tag{3}$$

where

$$f_0(x) = \left[1 + \exp\Big(\beta(x-1)\Big)\right]^{-1}, \tag{4a}$$

$$f_c(x) = \left[\frac{\mathrm{erf}(x)}{x}\right], \tag{4b}$$

$$f_{so}(x) = \left[x\cosh^2\Big(\beta(x-1)/2\Big)\right]^{-1}. \tag{4c}$$

The only model parameter that appears in these last expressions is $\beta = c/a$, which is defined as the ratio of the half density radius c to the diffuseness parameter a of the Wood-Saxon potential. With the exception of β, the mean-field potential depends linearly on two strength parameters λ_0 and λ_{so} for both neutrons and protons, and on one additional parameter λ_c for the protons. The linear dependence of the Hamiltonian on the model parameters is an important condition for the efficient performance of reduced basis emulators [6].

To determine the various model parameters across the nuclear chart we rely on the predictions of FSUGarnet [13], a realistic covariant energy density functional calibrated to the properties of finite nuclei and neutron stars. Effective non-relativistic "Schrödinger-like" central and spin-orbit potentials naturally emerge from such a description [14] and are plotted in Fig.1 for the case of ^{208}Pb. Without any further adjustments, a Woods-Saxon form and its associated derivative provide a highly accurate representation of the non-relativistic potentials. The proton fit to the central potential also includes a Coulomb contribution as in Eqs.(3-4). Note that for simplicity, we have assumed that both the half-density radius c and the diffuseness a of the spin-orbit potential are identical to the corresponding parameters of the central potential. Finally, we note that the effective Schrödinger-like central and spin-orbit potentials depend on energy [14], so we have fixed its value to an average binding energy of 40 MeV. Optimal values for the Woods-Saxon parameters for a variety of spherical nuclei are listed in Table I. In this first publication we highlight the power and flexibility of the approach by focusing on the neutron single-particle spectrum.

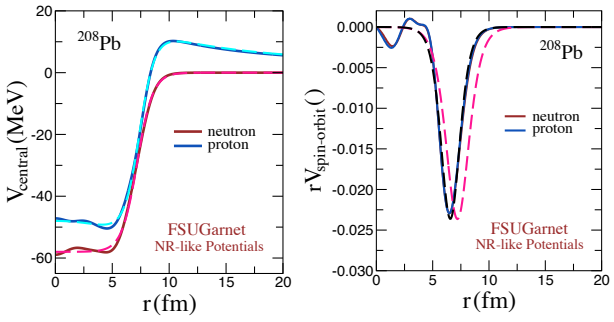


FIG. 1. Depicted by the solid lines are neutron and proton effective "Schrödinger-like" central and spin-orbit potentials for ^{208}Pb derived from the covariant energy density functional FSUGarnet [13]. The dashed lines represent the corresponding Woods-Saxon fits. The slightly offset dashed line represents a fit to the spin-orbit potential that uses the same half-density radius and diffuseness as the central potential.

Reduced basis methods will be compared against a conventional solution to Schrödinger's equation based on the Runge-Kutta algorithm. In this case, one uses the shooting method [15] to obtain all bound states that are supported by the assumed mean-field potential. For the construction of the reduced basis, the following procedure is implemented. First, we start by generating ten random triplets for the three dimensionless parameters listed in Table I, namely, λ_0, λ_{so}, and β. Given our goal of describing the entire single-particle spectrum for a variety of nuclei, those random values are drawn from a uniform distribution spanning the values listed in Table I. For example, for the central potential, random values are drawn from a uniform distribution within the $28.02 \leq \lambda_0 \leq 144.98$ interval. Second, we train the reduced basis model by obtaining exact solutions for each of the ten realizations by invoking the Runge-Kutta method. In this manner, one generates a trained set of (non-orthogonal) bound states for every angular momentum channel. Third, the optimal set of orthonormal basis functions is generated by filtering the (non-orthogonal) trained set through a singular value decomposition (SVD) routine. Finally, from such optimally generated set, one keeps the most important basis states as determined by their relative condition number. That is, one only keeps those basis states for which the ratio of its singular value to the corresponding largest singular value exceeds the arbitrarily chosen bound of 10^{-3}. This procedure generates reduced bases with dimensions ranging from as large as nine (for the $\kappa = -1$ sector) to as small as four (for the $\kappa = -7$ sector). Note that the binding energy is given in terms of dimensionless energy ε by $E_{bind} = \varepsilon V_0/\lambda_0$. It is important to underscore that by following such a procedure, we aspire to build a universal reduced basis that may be used without modification to generate all bound states—both ground and excited states—for all spherical nuclei. To our knowledge, the only extension of EC to excited states is the work by Franzke and collaborators that was applied to the one-dimensional quartic anharmonic oscillator [16].

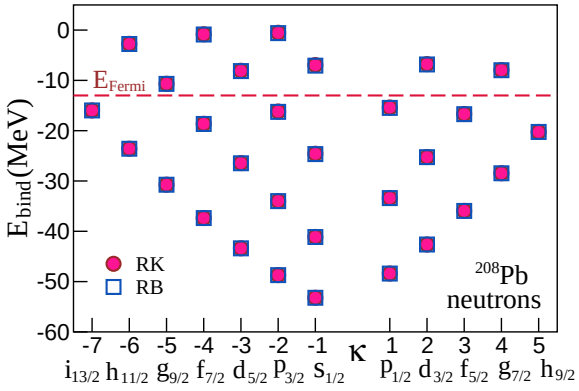


FIG. 2. The entire single-neutron spectrum of ^{208}Pb as generated by the mean-field potential listed in Table I. The circles are the results obtained with the Runge-Kutta (RK) algorithm while the squares are predictions using a well motivated reduced basis (RB). The dashed line indicates the Fermi energy separating the 22 occupied orbitals from the eight empty ones.

Besides the construction of a well-motivated basis that captures the essential physics, the reduced basis method also requires an efficient framework to solve the underlying set of dynamical equations. A powerful framework to do so, especially for systems of non-linear differential equations, is the Galerkin projection approach that determines the optimal set of expansion coefficients [5, 7, 8]. In our particular case, the Galerkin approach is equivalent to the direct diagonaliza-

Nucleus	V_0 (MeV)	V_{so}	c (fm)	a (fm)	λ_0	λ_{so}	β
^{16}O	62.232	0.03304	3.0551	0.66531	28.016	0.9608	4.5920
^{40}Ca	62.075	0.02558	4.2101	0.69815	53.067	1.0251	6.0303
^{48}Ca	61.339	0.03024	4.3166	0.66256	55.126	1.2425	6.5150
^{68}Ni	59.433	0.02748	4.9235	0.65209	69.486	1.2876	7.5502
^{90}Zr	59.981	0.02659	5.4609	0.67456	86.272	1.3820	8.0955
^{132}Sn	57.637	0.02662	6.13881	0.63767	104.76	1.5553	9.6269
^{208}Pb	57.996	0.02361	7.19934	0.68375	144.98	1.61791	10.529

TABLE I. Optimal central, spin orbit, half-density radius, and diffuseness Woods-Saxon parameters for a representative set of doubly-magic nuclei. The parameters were fitted to effective Schrödinger-like neutron potentials derived from a realistic covariant energy density functional [13]. The last three columns list the corresponding dimensionless parameters, as per Eqs.(3-4).

tion of the Hamiltonian matrix in the reduced basis space. Note that the diagonalization of the Hamiltonian must be done within each angular momentum subspace.

We display in Fig. 2 the bound state neutron spectrum for ^{208}Pb, generated by the exact Runge-Kutta algorithm (red circles) and the reduced basis method (blue squares). The agreement for both ground and excited states for all quantum numbers is excellent. Indeed, the root-mean-square error defined in terms of the total number of bound states N,

$$\varepsilon_{\rm rms} = \sqrt{\frac{1}{N}\sum_{n=1}^{N}\left(\varepsilon_n^{\rm (RK)} - \varepsilon_n^{\rm (RB)}\right)^2}, \qquad (5)$$

amounts to only $\varepsilon_{\rm rms} \approx 0.01$ MeV. The agreement is so good that one can only provide approximate rms-errors, as it is unlikely that our codes can compute bound-state energies with a precision of better than 10 keV. This suggests that the reduced basis could be made even smaller. The dashed line in Fig. 2 denotes the Fermi energy which divides the 22 occupied states from the 8 vacant (but still bound) single-particle orbitals. It is important to underscore that all states with the same angular momentum number κ—independent of the number of nodes—emerge directly from the diagonalization procedure within such an angular momentum sector. For example, in the $\kappa=-1$ ($l=0$, $j=1/2$) sector, the diagonalization of the 9×9 Hamiltonian matrix yields exactly four bounds-state energies that are in very close agreement with the predictions of the Runge-Kutta algorithm.

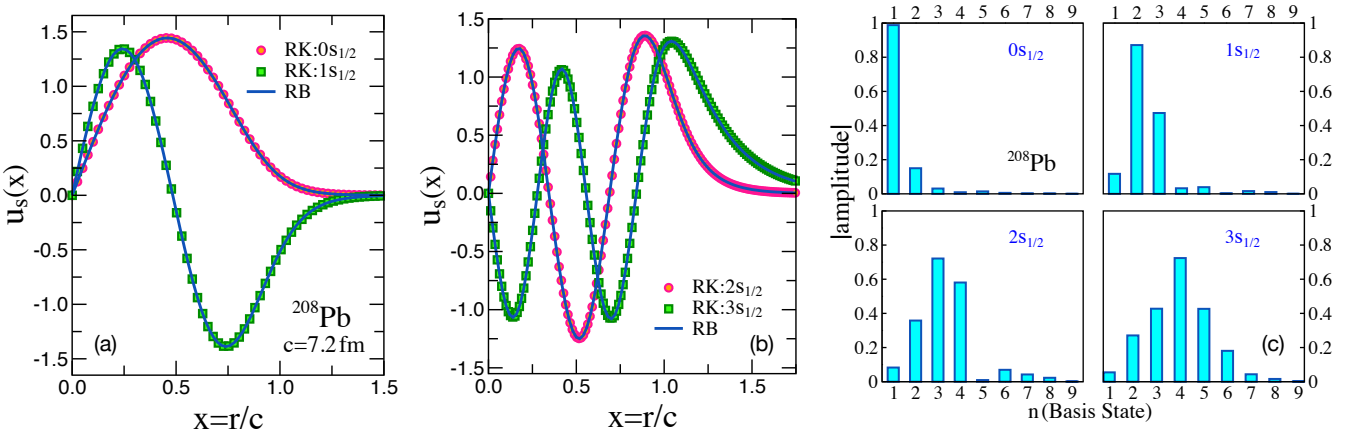


FIG. 3. The first two (a) and the next two (b) $S_{1/2}$ bound-state orbitals of ^{208}Pb as generated by the Runge-Kutta algorithm (circles/squares) and the reduced basis method (solid lines). Also shown in (c) are the absolute values of the projection amplitudes of all four states onto the $\kappa=-1$ reduced basis.

Although the agreement is excellent, predictions for energies tend to be more accurate than for other observables by virtue of the Raleigh-Ritz variational principle [17]. To ascertain that the success of the RBM goes beyond the bound-state energies, we have plotted in Fig. 3 the four $\kappa=-1$ bound-state wave-functions supported by the potential. In the figure the Runge-Kutta results are depicted with circles/squares and the corresponding predictions from the RBM with solid lines. Not only are the wave-functions accurately reproduced, but the efficiency of the reduced basis is exceptional. Indeed, also displayed in Fig. 3 are the absolute values of the projection amplitudes of all four states onto the $\kappa=-1$ reduced basis. The figure illustrates how a well motivated reduced basis with only nine (or even seven!) states can accurately and effi-

ciently reproduce the entire spectrum. In particular, the (nodeless) ground-state orbital can be essentially reproduced with only two basis states. To illustrate the universality of the basis, we now demonstrate that the same reduced basis without any additional modification can reproduce the single-particle spectrum of ^{48}Ca (with only 28 neutrons) as faithfully as in the case of ^{208}Pb (with 126 neutrons). That is, although the Hamiltonian matrix is nucleus dependent, the single-particle spectrum of ^{48}Ca is obtained by using the same exact basis as in the case of ^{208}Pb.

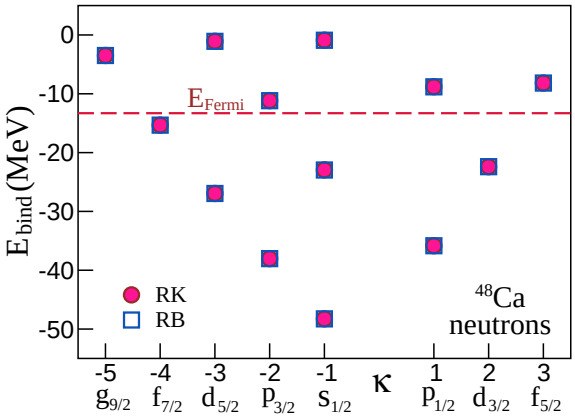


FIG. 4. The entire single-neutron spectrum of ^{48}Ca as generated by the mean-field potential listed in Table I. The circles are the results obtained with the Runge-Kutta algorithm while the squares are RBM predictions using a well motivated basis. The dashed line indicates the Fermi energy separating the seven occupied orbitals from the six empty ones.

The entire single-neutron spectrum for ^{48}Ca is shown in Fig. 4 using the same convention as in the case of ^{208}Pb. Again, the agreement between the exact results and the RBM predictions is excellent, even for the barely bound states. In this case the rms error is about $\varepsilon_{\rm rms} \approx 0.02$ MeV, although we reiterate that this is only an estimate since it is unlikely that we can compute bound-state energies with a precision of $\sim$10 keV. We observe that the efficiency of the reduced basis in this case is even more impressive than for ^{208}Pb. As shown in Fig. 5, not only are the two occupied $s_{1/2}$ states in ^{48}Ca accurately reproduced, but one can do so with essentially only one basis state, namely, with the one containing the correct number of nodes. Although the two lowest $s_{1/2}$ states emerge from the diagonalization of a 9×9 matrix, the scaling of the Hamiltonian by the half density radius guarantees that a very small number of basis states are required to reproduce the exact single-particle orbitals.

In summary, we have constructed a highly efficient and accurate reduced order model to emulate the single-particle structure of atomic nuclei. The underlying mean-field Hamiltonian is constrained by the predictions of a realistic energy density functional. The reduced basis was generated by filtering the trained set of eigenfunctions through a singular value decomposition routine. Although the universality of the reduced basis was demonstrated only for ^{48}Ca and ^{208}Pb, the accuracy of single-particle structure of all nuclei listed in Table I was verified without any modification to the basis. These results will be presented in a forthcoming publication [18]. To some extent, the success of the reduced basis method implemented here may be attributed to the simple scaling of the Hamiltonian. Although the half-density radius of the nuclei under consideration varies by more than a factor of two, the scaling leads to bound-state wave-functions that are highly similar to each other (see Figs. 3 and 5) practically guaranteeing the robustness of the reduced basis and the success of the approach.

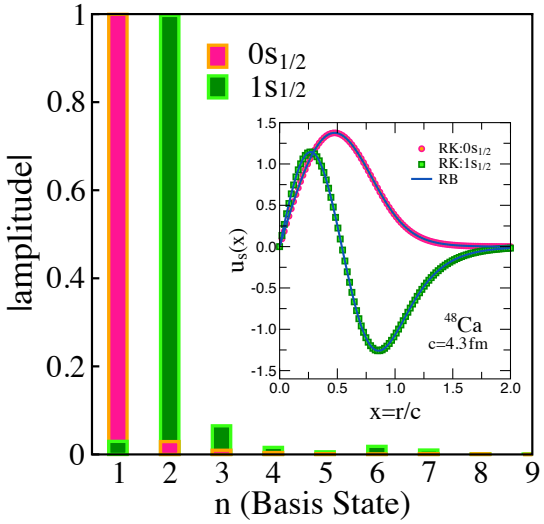


FIG. 5. The two occupied $s_{1/2}$ bound-state orbitals of ^{48}Ca as generated by the Runge-Kutta algorithm (circles/squares) and the reduced basis method (solid lines). Also shown are the absolute value of the projection amplitudes of the two states onto the $\kappa=-1$ reduced basis.

In a longer publication we will explore further the universality of the reduced basis by computing both neutron and proton single-particle spectra for a variety of nuclei [18]. We will quantify the improvement in speed of the RB emulator relative to the traditional RK solver. The highest computational burden is in generating the Hamiltonian matrix from the parameters specific to each nucleus. Although the reduced basis is universal, the entire matrix must be recalculated even if a single parameter in the Hamiltonian is changed. In principle, the efficiency may be increased if some of the matrix elements could be calculated in advance and stored offline, thereby reducing the computational burden. However, this is only feasible if the potential is linear in all of the parameters. Yet, as shown in Eqs.(3-4), the potential depends non-linearly on the nucleus-specific parameter β, a relatively large quantity that is defined as the ratio of the half density radius to the diffuseness parameter. However, for the range of values of interest, the dimensionless Woods-Saxon form $f_0(x;\beta)$ may be linearized using the Empirical Interpolation Method (EIM) [6] as follows:

$$f_0(x;\beta) \approx \sum_{m=1}^{M} b_m(\beta) f_m(x), \tag{6}$$

where the functions $f_m(x)$ may be obtained following a pro-

cedure analogous to the one used to extract the reduced basis. That is, one generates Wood-Saxon potentials $f_0(x;\beta)$ for different values of the parameters β and then performs a singular value decomposition to identify and retain the M most important components. The nucleus-specific information is encoded in the coefficients $b_m(\beta)$ that may be determined by solving a set of M linear equations after identifying the various optimal locations x, usually chosen by a greedy algorithm scheme [6]. Once the Hamiltonian has been fully linearized, matrix elements of the various components of the potential energy can be evaluated once (the offline stage) and then stored for later use (the online stage) to compute the spectrum of all nuclei of interest. Our ultimate goal is to build a reduced order framework to accurately and efficiently calibrate modern energy density functionals for which Bayesian optimization is demanded. This requires many samplings of a large number of observables in order to properly quantify correlations and model uncertainties. The computational burden is high, but it can be mitigated by using emulators which, as we have shown here, reproduce the behavior of the high-fidelity model with remarkable accuracy at a fraction of the computational cost.

ACKNOWLEDGMENTS

We are grateful to Pablo Giuliani for his guidance, many stimulating discussions, and a thorough reading of the manuscript. This material is based upon work supported by the U.S. Department of Energy Office of Science, Office of Nuclear Physics under Award Number DE-FG02-92ER40750.

[1] D. Frame, R. He, I. Ipsen, D. Lee, D. Lee, and E. Rrapaj, Phys. Rev. Lett. **121**, 032501 (2018).
[2] S. König, A. Ekström, K. Hebeler, D. Lee, and A. Schwenk, Phys. Lett. B **810**, 135814 (2020).
[3] R. J. Furnstahl, A. J. Garcia, P. J. Millican, and X. Zhang, Phys. Lett. B **809**, 135719 (2020).
[4] C. Drischler, M. Quinonez, P. G. Giuliani, A. E. Lovell, and F. M. Nunes, Phys. Lett. B **823**, 136777 (2021).
[5] A. Quarteroni, A. Manzoni, and F. Negri, *Reduced Basis Methods for Partial Differential Equations: An Introduction*, Vol. 92 (Springer, 2015).
[6] J. S. Hesthaven, G. Rozza, and B. Stamm, "Certified reduced basis methods for parametrized partial differential equations," (Springer, Switzerland, 2016).
[7] E. Bonilla, P. Giuliani, K. Godbey, and D. Lee, (2022), arXiv:2203.05284 [nucl-th].
[8] J. A. Melendez, C. Drischler, R. J. Furnstahl, A. J. Garcia, and X. Zhang, (2022), arXiv:2203.05528 [nucl-th].
[9] P. Benner, W. Schilders, S. Grivet-Talocia, A. Quarteroni, G. Rozza, and L. Silveira, "Model order reduction: Applications," (De Gruyter, 2020).
[10] A. Bohr and B. R. Mottelson, "Nuclear structure," (World Scientific Publishing Company, New Jersey, 1998).
[11] B. R. Barrett, P. Navratil, and J. P. Vary, Prog. Part. Nucl. Phys. **69**, 131 (2013).
[12] G. Hagen, T. Papenbrock, M. Hjorth-Jensen, and D. J. Dean, Rept. Prog. Phys. **77**, 096302 (2014).
[13] W.-C. Chen and J. Piekarewicz, Phys. Lett. **B748**, 284 (2015).
[14] R. D. Amado, J. Piekarewicz, D. A. Sparrow, and J. A. Mcneil, Phys. Rev. C **28**, 1663 (1983).
[15] W. H. Press, B. P. Flannery, S. A. Teukolsky, and W. T. Vetterling, "Numerical recipes: The art of scientific computing," (Cambridge University Press, 1989).
[16] M. C. Franzke, A. Tichai, K. Hebeler, and A. Schwenk, Phys. Lett. B **830**, 137101 (2022).
[17] R. P. Feynman and A. R. Hibbs, "Quantum mechanics and path integrals," (Dover Publications, New York, 2010).
[18] A. L. Anderson and J. Piekarewicz, Phys. Rev. C. (2022), in preparation.